Urban Forestry & Urban Greening 86 (2023) 128017

Contents lists available at ScienceDirect

Urban Forestry & Urban Greening

journal homepage: www.elsevier.com/locate/ufug

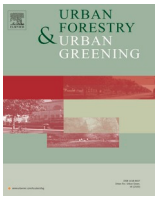

Optimization of tree locations to reduce human heat stress in an urban park

Tongping Hao [a,b], Qunshan Zhao [c,*], Jianxiang Huang [a,b,**]

[a] Department of Urban Planning and Design, The University of Hong Kong, 8/F Knowles Building, Pokfulam Road, Hong Kong Special Administrative Region of China
[b] The University of Hong Kong Shenzhen Institute of Research and Innovation, 5/F, Key Laboratory Platform Building, Shenzhen Virtual University Park, No.6, Yuexing 2nd Rd., Nanshan, Shenzhen 518057, China
[c] Urban Big Data Centre, School of Social and Political Sciences, University of Glasgow, Glasgow G12 8RZ, UK

ARTICLE INFO

Keywords:
Human thermal comfort
Location modeling and optimization
Microclimate simulation
Tree location
Tree arrangement
Urban heat

ABSTRACT

Trees provide cooling benefits through shading and evapotranspiration; they are regarded as an important measure in heat-resilient urban planning and policies. Knowing where to plant trees for maximum cooling benefits, given practical and resource constraints, remains a challenge in both practice and research. Literature in the field of tree modeling and location optimization is limited, either by the incompleteness in accounting for tree shading, evapotranspiration, and the modifying effect of wind, or by the slow-running speed of the Computational Fluid Dynamics model, making them less applicable in practice. This paper describes a novel method to search for the optimal locations for trees to maximize their cooling benefits in an urban environment. A rapid simulation model was applied to assess on-site heat stress under the influences of trees, which was evaluated using field measurements conducted under hot, temperate, and cool weather conditions in an urban park in Hong Kong. It was then linked to a genetic algorithm in search of a near-optimal tree layout. The proposed method was tested in the same park, and it can automatically identify locations to plant new trees to minimize heat stress, subject to practical constraints such as avoiding existing buildings and utilities. It can also identify the optimal locations to rearrange the existing 55 trees, hypothetically, which can cool the park by up to 0.3 ℃ in on-site average equivalent temperature compared with the worse scenario. Trees can cool the most if they are concentrated on the leeward side of the park, rather than spread evenly. The proposed method runs significantly faster than existing approaches, and it can inform research and landscape design practices concerning park cooling as a goal.

1. Introduction

Trees are considered a time-tested cooling strategy in hot climates. Tree canopies shade pedestrians from direct sunlight, and the evapotranspiration of tree leaves can reduce the ambient air temperature (Oke, 1989; Wong et al., 2021). For this reason, trees are often considered a high priority in heat-resilient urban policy to mitigate weather extremes and urban heat island effects. Examples include multiple policy addresses by the Hong Kong government (HKG, 2022), pledging millions of trees to be planted within the city limits. Similarly, Singapore's Green Plan 2030 has designated some 200 ha of urban land as nature parks (SG, 2021). Other municipal policies have established quantitative targets, such as the 25% in tree coverage pledged by the Tree and Shade Master Plan of Phoenix, USA (City of Phoenix, 2010), or 30% suggested by the 2030–50 Master Plan for Kuala Lumpur, Malaysia (Kuala Lumpur City Hall, 2021) and the 2017–37 Master Plan for Barcelona, Spain (City of Barcelona, 2017). Melbourne, Australia has set a more ambitious target of 40% (City of Melbourne, 2012).

Existing policies fail to mention where to plant trees. The number of trees allowable is often constrained by the ground surface area available for planting and the maintenance budget for irrigation, pest control, trimming, etc. Landscape designers are therefore confronted with the challenge to achieve more cooling with fewer trees, and there is little consensus in research or practice on how to achieve this. For instance, literature disagreed upon whether to concentrate trees in a few locations or to spread them thinly across a larger area for maximum cooling benefits (Morakinyo and Lam, 2016; Zhang et al., 2018; Zhao et al., 2018). Placing trees in breezeways, concluded by a recent study by Huang et al. (2022), can further reduce the in-situ pedestrian heat stress

* Corresponding author.
** Correspondence to: Department of Urban Planning and Design, 8/F Knowles Building, The University of Hong Kong, Pokfulam Road, Hong Kong Special Administrative Region of China.
E-mail addresses: Qunshan.Zhao@glasgow.ac.uk (Q. Zhao), jxhuang@hku.hk (J. Huang).

https://doi.org/10.1016/j.ufug.2023.128017
Received 30 November 2022; Received in revised form 24 June 2023; Accepted 27 June 2023
Available online 29 June 2023

Nomenclature

List of symbols

a_p	Absorption coefficient of solar radiation for a person.
A_{ij}	Area of zone opening (m^2).
C_P	Specific heat capacity (J/kg).
E_g	Long-wave radiation intensity of the ground surface (W/m^2).
E_{sky}	Long-wave radiation intensity of the sky (W/m^2).
E_{sol}	Solar radiation intensity (W/m^2).
ET_0	Rate of plant evapotranspiration (m/s).
E_w	Long-wave radiation intensity of a surrounding wall (W/m^2).
$F_{g\to p}$	View factor between the ground surface and a person (ratio, 0–1).
$F_{sky\to p}$	View factor between the visible sky and a person (ratio, 0–1).
$F_{sol\to p}$	View factor between the short-wave sources and a person (ratio, 0–1).
$F_{w\to p}$	View factor between a surrounding wall and a person (ratio, 0–1).
F_{ij}	Zonal airflow rate from zone j to i (kg/s).
F_{ji}	Zonal airflow rate from zone i to j (kg/s).
G	Soil heat flux density at the soil surface (W/m^2).
H_z	Vertical elevation at height z (m).
L_w	Latent heat of water (2.43×10^6 J/kg).
J	Number of neighboring zones.
P_a	Measured barometric pressure under the temperature T_a at operational weather station (Pa).
P_a^s	Static air pressure at any given height can be inferred from an operational weather station after adjusting for the stacking effect due to gravity (Pa).
P_{v_z}	Wind pressure at z m level (Pa).
$P_{v_{10}}$	Wind pressure at the boundary surfaces of the model domain at the 10 m level (Pa).
q_G^{ET}	Rate of latent heat absorption from greenery (W).
r_a	Aerodynamic resistance of the vegetation and soil surfaces (s/m).
r_s	Stomatal resistance of the vegetation and soil surfaces (s/m).
R	Energy gained from radiation (W).
$R_\uparrow$	Outgoing long-wave radiation from the plant surface (W/m^2).
$R_\downarrow$	Incoming radiation at the plant surfaces (W/m^2).
RH	Relative humidity (%).
T_a	Air temperature (K).
T_{a_i}	Uniform air temperature (K).
T_{mrt}	The localized mean radiant temperature (K).
TR_s	Transmissivity of a tree canopy in the short-wave spectrum.
TR_l	Transmissivity of a tree canopy in the long-wave spectrum.
P_i	Uniform air pressure (Pa).
R_a	Gas constant for air.
S_{sk}	Energy loss via sweat secretion (W).
$V_{1.5}$	Wind speed at a reference height of 1.5 m (m/s).
V_{10}	Wind speed at a reference height of 10 m (m/s).
V_a	Wind speed (m/s).
V_i	Zonal volume (m^3).
V_p	Air velocity perpendicular to the zone surface after adjusting for vertical profile (m/s).
Δ	Slope of the saturation vapor pressure-temperature curve (Pa/K).
ΔT_{a_i}	Zonal air temperature change within a small-time interval Δt (K).
ε_g	Emissivity of the ground surface (ratio, 0–1).
ε_{sky}	Emissivity of the sky (ratio, 0–1).
ε_w	Emissivity of the a surrounding wall (ratio, 0–1).
δ_ε	Vapor pressure deficit (Pa).
γ	Psychrometric constant (66 Pa/K).
σ	Stephan-Boltzmann Constant ($\sigma = 5.67\times10^{-8}$ W/m^2 K^4).
ρ_{a_i}	Uniform air density (kg/m^3).
φ_{i_n}	Absolute humidity of zone i at the time step n.

in a high-density city compared with those planted elsewhere. Rooftop trees, on the other hand, have a negligible cooling effect at the ground level where pedestrian activities concentrate (Ng et al., 2012). The research findings above often depend on the study context and cannot be readily implemented. In practice, such decisions were often left to rules-of-thumb principles, personal experience, intuitions, or made opportunistically, i.e., to place trees in avoidance of buildings and infrastructure, or away from underground utilities for unhindered root development. Some decisions cited the pre-modern Chinese practices of Fengshui (Mak and Ng, 2005) or its Indian equivalence of Vaastu Shastra (Patra, 2009), with little support from research evidence. There is a need for a systematic approach to identifying optimal tree locations for urban cooling.

Research literature stopped short of providing a design tool to locate trees to maximize their cooling benefits at the micro-scale. The majority of simulation models have missed one or a few components of tree cooling mechanisms, such as shading, evapotranspiration, and the modification of localized wind near a tree canopy (Buccolieri et al., 2018; Yang et al., 2019). Of a handful of attempts made to link the tree simulation model with optimization algorithms (Park et al., 2020; Stojakovic et al., 2020; Wallenberg et al., 2022; Zhao et al., 2017), yet they tend to be limited by the lack of one or several tree cooling components, or their slow computational speed which prevented them from achieving meaningful optimal. Thus, new methods of modeling are needed for not only a rapid and reliable prediction of trees' cooling benefits but also an efficient integration with optimization models. Another body of literature, which has recently flourished in the domain of urban climate (Ng et al., 2012; Ng and Ren, 2018; Yuan et al., 2017) and geography (Cheung et al., 2020; Li and Song, 2019; Morakinyo et al., 2020; Zhang and Gou, 2021), has extensively studied the cooling benefit of trees in urban environments. However, the spatial resolutions of the above models (~1 km) are often too coarse to address the challenge of determining where to plant each individual tree. Questions remain as to whether tree locations can be optimized mathematically based on simulation models, and if yes, what lesson does it afford to heat-resilient urban policies and landscape design practices?

This paper describes a novel method to optimize tree locations for urban cooling. The aim is to identify a systematic approach in search of optimal tree locations to reduce human heat stress in outdoor spaces. The objectives are to 1) develop a rapid simulation model for assessing the cooling effects of trees with the support of field validation to verify the proposed method; 2) integrate the simulation model with an optimization algorithm to identify optimal tree locations; and 3) test the method in an urban park with practical design constraints. Field measurements were conducted in a large, vegetated urban park in Hong Kong, and the results were used to evaluate the simulation model. This model was then used to automatically identify optimal tree locations given practical constraints. The implications for urban forestry practices and landscape design were discussed concerning cooling performances as a goal.

2. Literature review

2.1. Tree modeling

The cooling effects of trees have been studied extensively. A large body of modeling literature relied on energy and mass conservation equations to assess the shading effect, evapotranspiration, and the modifying effect of wind.

The shading effects of trees have been considerably investigated using numerical models. ENVI-met is a popular commercial software in the study of vegetated urban microclimate (Bruse and Fleer, 1998). The software allows for the input of tree data as 3D geometries of multiple layers, each is assigned a leaf area density value in order to calculate the absorption of solar radiation. A primary drawback of ENVI-met, despite merit, is its slow running speed and the complex input setting of individual trees (Liu et al., 2021; Toparlar et al., 2017), which make it difficult to be coupled with an optimization algorithm to identify the optimal tree locations. Similar approaches have been adopted by SOLWEIG (Lindberg and Grimmond, 2011), which models the shading effect of trees using pre-assigned transmission factors for tree canopies. Other studies, such as those by Krayenhoff et al. (2014) and Park et al. (2018), follow similar principles. A more reliable method for accounting for shading is the ray-tracing algorithm. Examples include the CityComfort+ method by Huang et al. (2014) based on inverse ray-tracing algorithms, which accounts for the direct, diffuse, and reflected solar radiation as well as long-wave radiation from the atmosphere and solid surfaces. Another study is the TUF-Pedestrian by Lachapelle et al., (2021), which uses ray-tracing algorithms to simulate radiative flux in a vegetated urban environment.

The modifying effect of wind by tree canopies has been primarily assessed using computational fluid dynamics (CFD) methods (Krayenhoff et al., 2015). A tree canopy is first characterized as a porous medium, with cells assigned with leaf area density attributes. It is then placed in the CFD domain, with pre-defined boundary conditions, drag coefficients, and turbulence models. Examples include the study by Krayenhoff et al. (2015), which calculates spatial-averaged impacts of trees on airflow in the urban canopy, governed by drag coefficients and turbulence length scales derived from a CFD-based model, and the study by Redon et al. (2019), which uses source terms to calculate the turbulent flux modified by vegetation in the urban canopy. A large number of CFD software are equipped with modules for such a purpose, including ENVI-met (2023), OpenFOAM (2022), Ansys Fluent (2022), PHOENICS (2022). Non-CFD approaches have also been developed, although less common, based on first-principles models, i.e., solving energy balance equations at various scales (Redon et al., 2019).

The evapotranspiration of trees has been studied initially in agriculture and later in built-environment literature. Existing models rely on empirically derived equations, including the Penman-Monteith Equation and its variations (Allen et al., 1998; Duursma and Medlyn, 2012), which express the intensity of plant evapotranspiration as a function of the intrinsic properties of species and meteorological conditions such as solar radiation, air temperature, humidity, wind speed, etc. These have been incorporated in more recent studies on the interactions between trees and the surrounding urban environment. For instance, Huang et al. (2022) developed the Urban Greenery and Built Environment model to assess street-scale temperature and human heat stress under the influences of greenery, and the model has been subsequently evaluated using field measurement data collected from Hong Kong. Similar approaches include the VTUF-3D model by Nice et al. (2018), the TEB-SURFEX model by Redon et al. (2019), the BEP-Tree model by Krayenhoff et al. (2020), and the Urban Ecohydrological Model (UT&C v1.0) by Meili et al. (2021). Some commercial CFD software, such as ENVI-met, OpenFOAM, and PHOENICS, have also embedded vegetation modules in their algorithms to assess the evapotranspiration of plants in an urban environment, although their approach is not fully transparent to researchers due to the black-box nature of commercial software.

Tangential to the tree models above, a large body of literature focuses on using thermal remote sensing to study the cooling effect of vegetation cover at urban and regional scales. Notable examples include those by Fan and Wang (2020) and by Zhao et al. (2015), which use land surface temperature data obtained from satellite infrared thermography.

2.2. Tree location optimization

Simulation-based optimization studies have made significant advancements in the last two decades. Successful applications have been achieved in the field of building energy, structural engineering, and semiconductors, etc., in which digital tools were used in search of optimal design under given objectives and constraints. However, research literature on optimizing tree locations for cooling performances is limited. An exhaustive search in scientific publications in the last two decades yielded four studies: the first by Chen et al. (2008) pioneered an optimization algorithm based on CFD models to identify the optimal design for buildings and trees to reduce human heat stress. They deployed a two-step optimization workflow to reduce the computational load, first relying on a coarse CFD mesh for quick calculation and screening, followed by a refined CFD simulation to identify the optimal design. The remaining three studies by Bajsanski et al. (2016), Zhao et al. (2017), and Milošević et al. (2017) adopted the brute-force method to identify the optimal tree layout for a single building or on a street segment, aiming to maximize shade coverage, reducing the solar intensity, and mitigating human heat stress. However, none of these studies were able to exhaustively test all possible tree locations, as the number of alternatives tends to grow exponentially with the increase of design variables.

A parallel school of studies has achieved 'quasi-optimization,' which is based either on an 'incomplete' simulation for tree cooling mechanism or a compromised optimization method. For instance, Stojakovic et al. (2020) used the mean radiant temperature (MRT) as the objective to optimize tree locations, while other cooling mechanisms, such as evapotranspiration and the modifying effect of wind, have not been accounted for. Based on the same MRT objective, Park et al. (2020) and Wallenberg et al. (2022) obtained similar results, and their findings may suffer from the same limitations. Another body of literature used multi-scenario comparisons to identify tree locations with superior cooling performances. Strictly speaking, these are not optimizations, although the term tends to be used loosely. For instance, Morakinyo and Lam (2016) compared the simulated cooling performance of a double-row tree arrangement with a single-row alternative, they concluded that the former is more effective in reducing pedestrian heat stress. Zhang et al. (2018) compared the cooling performances of three alternative tree layouts of the same green coverage ratio, from sparsely distributed to densely packed; they found that sparsely planted trees outperformed the other two in reducing human heat stress.

2.3. Research gap

In sum, relevant research is limited mainly in two aspects. First, literature in the field of tree modeling and optimization has fallen short in providing a reliable and computationally efficient tool. Many tree models rely on computationally expensive CFD methods, which cannot be easily coupled with optimization algorithms. This limitation has left researchers with an undesirable trade-off, of either choosing an overly simplified simulation model missing one or a few components of tree cooling mechanisms, such as shading, evapotranspiration, and the modification of localized wind near a tree canopy, or settling with sub-optimal with reduced optimization runs. Of a handful of attempts made to link the tree simulation model with optimization algorithms (Park et al., 2020; Stojakovic et al., 2020; Wallenberg et al., 2022; Zhao et al., 2017), their results tend to suffer from the lack of various tree cooling components or their slow computational speed which prevented them from achieving meaningful optimal. Thus, there is a need for a

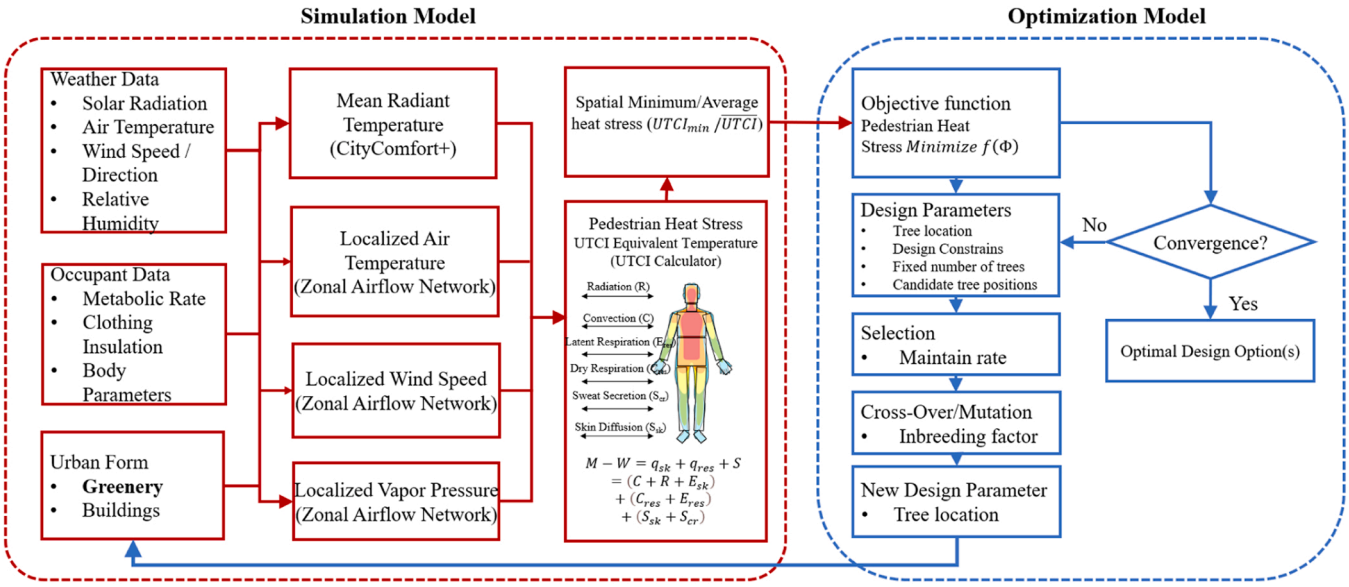

Fig. 1. A conceptual framework of the simulation-based optimization for tree cooling, developed based on an earlier study by Hao et al. (2022).

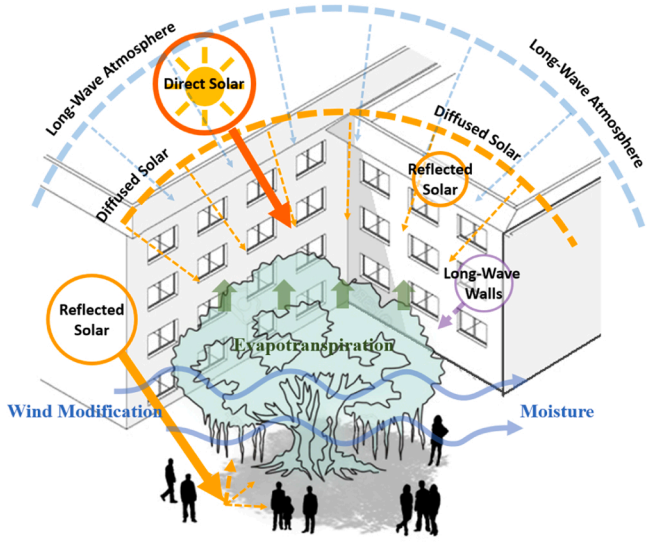

Fig. 2. A conceptual illustration of the cooling components of a tree canopy in outdoor spaces. The shading effects are modeled based on direct, diffused, reflected solar radiation and long-wave radiation from the atmosphere and surrounding walls; the evapotranspiration is calculated using the Penman-Monteith formula; while the wind modification and the moisture impacts are calculated using a zonal airflow network model.

computationally efficient simulation model to assess the cooling performances of tree canopies in outdoor spaces, together with a systematic approach to searching for optimal tree locations to maximize the cooling potentials of urban greenery.

Research evidence remains thin on tree cooling with respect to their locations relative to the surrounding context and each other. Instead, the majority of literature tend to focus on the cooling performance in relation to tree coverage ratio (Yang et al., 2017), tree species (Li et al., 2021; Morakinyo et al., 2020), canopy characteristics (Zhang and Gou, 2021), or the maintenance factors of urban greenery (Li and Song, 2019). There is a need for a refined understanding of the cooling benefits associated with the location of trees, rather than their quantities.

3. Methods

A novel method is developed to optimize tree locations for urban cooling. The aim is to identify a systematic approach in search of optimal tree locations to reduce human heat stress in an outdoor space. A rapid simulation model was first developed and evaluated to assess the cooling performances of tree canopies; the model was then integrated with an optimization algorithm in search of optimal tree locations. The above method is illustrated in Fig. 1, and it has been tested in a large Urban Park in Hong Kong. The optimization process is a cooling performance-driven process, which frequently calls to the simulation-based objective function. The performances of design options were assessed by the simulation model, with a certain percentage of those performing highly to be selected as parents to produce the new generation. The process was repeated until the convergence criteria were achieved, defined as no improvement in cooling performance observed over pre-defined maximum generations.

3.1. Tree simulation model

A tree canopy modifies the micro-scale thermal environment through shading, evapotranspiration, and the modification of wind. A first-principles simulation model was applied in this study to assess the cooling effect of tree canopies in outdoor spaces, which accounts for all the above cooling mechanisms of a tree canopy (Fig. 2). The quantitative assessment of each mechanism and their combined influences on human perception of heat stress are specified in the following step.

The shading effects of a tree canopy and the interactions with urban surfaces at the short-wave and long-wave spectrum are modeled using the inverse ray-tracing method. The inputs are tree canopies simplified as layered geometries, the canopy/leaf transmissivity, and the building massing and surface thermal properties such as albedo, emissivity, and thermal mass. The output is the Mean Radiant Temperature (T_{mrt}) received at the human scale, defined as the uniform temperature of an imaginary enclosure in which the radiant heat transfer from the human body is equal to the radiant heat transfer in the outdoor space. T_{mrt} under a tree canopy is expressed as a function of direct, diffused, reflected solar radiation as well as long-wave radiation from the atmosphere and surrounding walls and the ground (Eq. (1)). The modeling of T_{mrt} adapted an approach previously developed and validated in field measurements by Huang et al. (2014).

$$T_{\mathrm{mrt}} = \sqrt[4]{\frac{1}{\sigma}\left(TR_s \quad a_p \quad E_{sol} \quad \mathrm{F}_{\mathrm{sol}\to p} \quad + \quad TR_l \quad \varepsilon_{\mathrm{sky}} \quad E_{\mathrm{sky}} \quad \mathrm{F}_{\mathrm{sky}\to p} \quad + \quad \varepsilon_{\mathrm{w}} \quad E_{\mathrm{w}} \quad \mathrm{F}_{w\to p} + \varepsilon_{\mathrm{g}} \quad E_{\mathrm{g}}\cdot \mathrm{F}_{g\to p}\right)} \tag{1}$$

where σ is the Stephan-Boltzmann Constant (5.67 ×10 −8 W/m^2 K^4); TR_s is the transmissivity of a tree canopy in the short-wave spectrum; a_p is the absorption coefficient of solar radiation for a person (0.7); E_{sol} is solar radiation intensity (W/m^2); $F_{sol\to p}$ is the view factor between the short-wave sources and a person (ratio); TR_l is the transmissivity of a tree canopy in the long-wave spectrum; ε_{sky} is the sky emissivity (ratio); E_{sky} is the long-wave radiation intensity of the sky (W/m^2); $F_{sky\to p}$ is the view factor between the visible sky and a person (ratio); ε_w is the emissivity of a surrounding wall, with its long-wave radiation intensity denoted as E_w (W/m^2), and the view factor from the person as $F_{w\to p}$; ε_g , E_g, and $F_{g\to p}$ are the emissivity, long-wave radiation intensity, and view factor of the ground surface respectively.

The airflow and temperature profiles under and surrounding a tree are modeled using a zonal airflow network model. The pressure and temperature boundary conditions are determined using a nested CFD model within a larger domain containing the study area, which uses input parameters from nearby meteorological weather stations. A tree canopy was regarded as a porous media, which partially blocks wind and lowers the nearby air temperature through the absorption of latent heat, a process known as evapotranspiration. The porosity, which measures a percentage of the openings area of a surface over the total area, depends on tree species and their growth status according to literature (Bean et al., 1975). The model domain consists of a network of interconnected zones, each assumed of uniform zonal air temperature (T_{a_i}), density (ρ_{a_i}), and pressure (P_i) at a specific timestep. The ideal gas law in Eq. (2) (R_a is the gas constant for air). Zonal airflow rate F_{ij} (kg/s) from zone i to j can be expressed as a function (Eq. (3)) of pressure and density differences at the border and characteristics of the opening (A_{ij})

$$\rho_{a_i} = P_i / R_a T_{a_i} \tag{2}$$

The zonal pressure, air flow, and air temperature are governed by pressure balance, mass, and energy conservation equations, as expressed in Eqs. (3) – (5).

$$F_{ij} = f[\Delta P_{ij}, \Delta\rho_{ij}, A_{ij}] \tag{3}$$

$$\sum_{j=1}^{J} F_{i,j} = 0 \tag{4}$$

$$\sum_{j=1}^{J} C_p F_{ji}\left(T_j - T_i\right) + \frac{\Delta T_{a_i}}{\Delta t} C_p \rho_i V_i - q_G^{ET} = 0 \tag{5}$$

where F_{ij} and F_{ji} are the rate of the airflow (kg/s) between zone i and neighboring zone j; J is the number of neighboring zones; ΔT_{a_i} is the zonal air temperature change (K) within a small time interval Δt; C_P is the specific heat capacity (J/kg); V_i is and zonal volume (m^3); q_G^{ET} is the rate of latent heat absorption from greenery (W), to be estimated in Eq. (6).

The rate of latent heat absorption (q_G^{ET}) from a tree canopy was modeled using the Penman-Monteith formula (Allen et al., 1998). This approach has been previously evaluated in field studies using infrared thermal imaging of tree leaves in Hong Kong (Huang et al., 2022). q_G^{ET} can be expressed a function of ambient radiation, air temperature, humidity, and soil conditions (Eq. (6))

$$q_G^{ET} = L_w\, ET_0 = L_w \frac{\Delta(R_\downarrow - R_\uparrow - G) + \frac{\rho_a C_p (e_s - e_a)}{r_a}}{\Delta + \gamma\left(1 + \frac{r_s}{r_a}\right)} \tag{6}$$

where L_w is the latent heat of water (2.43 ×10^6 J/kg); ET_0 is the rate of evapotranspiration (kg/s); Δ is the slope of the saturation vapor pressure-temperature curve (Pa/K), to be calculated from air temperature T_{a_i}, given by Eq. (7).

$$\Delta = \frac{4098\left[0.6108\exp\left(\frac{17.27T_{a_i}}{T_{a_i}+237.3}\right)\right]}{\left(T_{a_i}+237.3\right)^2} \tag{7}$$

$R_\downarrow$ is the incoming radiation at the vegetation surfaces (W/m^2), to be estimated using the proposed tree simulation model; $R_\uparrow$ is the outgoing long-wave radiation from the plant surface (W/m^2), to be estimated using Stefan-Boltzmann's law; σ is the Stephan-Boltzmann Constant (σ =5.67 ×10^{-8} W/m^2 K^4); G is soil heat flux density at the soil surface (W/m^2); ρ_a is the density of the air (ρ_a = 1.27kg/m^3); C_p is the specific heat of the air (C_p = 1013 J/kg K); e_s is the saturation pressure (Pa) and e_a is actual vapor pressure (Pa); γ is Psychrometric Constant (66 Pa/K); r_s is the stomatal resistance, estimated as $r_s = r_1/LAI_{act}$ where r_1 is the stomatal resistance of the leaf (100 s/m for well-watered plants) and LAI_{act} is the Active Leaf Area Index (LAI), estimated as $LAI_{act} = 0.5 * LAI$; r_a is the aerodynamic resistance of the vegetation and soil surfaces, given by Eq. (7)

$$r_a = \frac{\ln\left[\frac{Z_w - d}{Z_{om}}\right]\ln\left[\frac{Z_h - d}{Z_{oh}}\right]}{k^2 V_z} \tag{8}$$

where Z_w and Z_h are the height of wind and humidity measurement above the ground; d is the height of the Zero Plane Displacement of the vegetated surface, estimated as two thirds of the vegetation height (h) ($d = 2/3h$); Z_{om} and $Z_{oh}$is the surface roughness length governing the momentum transfer and the heat/vapor transfer respectively, which can be simplified as $Z_{om} = 0.123 * h$ and $Z_{oh} = 0.1 * Z_{om}$; k is the Von Karman's Constant (0.41); V_z is the wind speed measured at the height of z above the ground.

The moisture field under and near a tree canopy is modeled using mass transfer equations, in which the tree leaves are treated as sources, with a computed intensity of ET_0. Water vapors are treated as a passive scalar to be transported along with airflow, governed by mass conservation. The changes of absolute humidity in zone i between timestep n and n-1 ($\varphi_{i_n} - \varphi_{i_{n-1}}$) equals the gains of which from sources and incoming airflow, minus the losses from outgoing airflow

$$\frac{(\varphi_{i_n} - \varphi_{i_{n-1}})V_i}{\Delta t} = N * ET_0 + \sum_{k=1}^{K} \varphi_{k_{n-1}} F_{k,i} - \sum_{j=1}^{J} \varphi_{i_{n-1}} F_{i,j} \tag{9}$$

where N is the number of tree canopies inside zone i; V_i is the volume of air in zone i; J is the number of zones to its downwind, and K to its upwind. $\varphi_{i_{n-1}}$ and $\varphi_{k_{n-1}}$ are the absolute humidity of zone i and the neighboring zone k at the previous time step $n-1$; Δt is a minuscule time lag between timestep n and n-1; $F_{i,j}$ is the outgoing airflow from zone i to j (m^3/s); $F_{k,i}$ is the incoming airflow from zone i to j (m^3/s); the calculations of $F_{i,j}$, $F_{k,i}$ are specified in the air and energy flow equations above.

The **perceived heat stress** of an occupant of an outdoor space was assessed using the Universal Thermal Climate Index (UTCI), a human bio-meteorological indicator. The UTCI accounts for human body energy balance under radiative, convective, and conductive heat transfer with the surrounding environment, it also models the thermal regulatory responses based on laboratory-based datasets (Jendritzky et al., 2012). The intensity of heat stress (UTCI) can be expressed as a function of localized air temperature (T_a), mean radiant temperature (T_{mrt}), relative

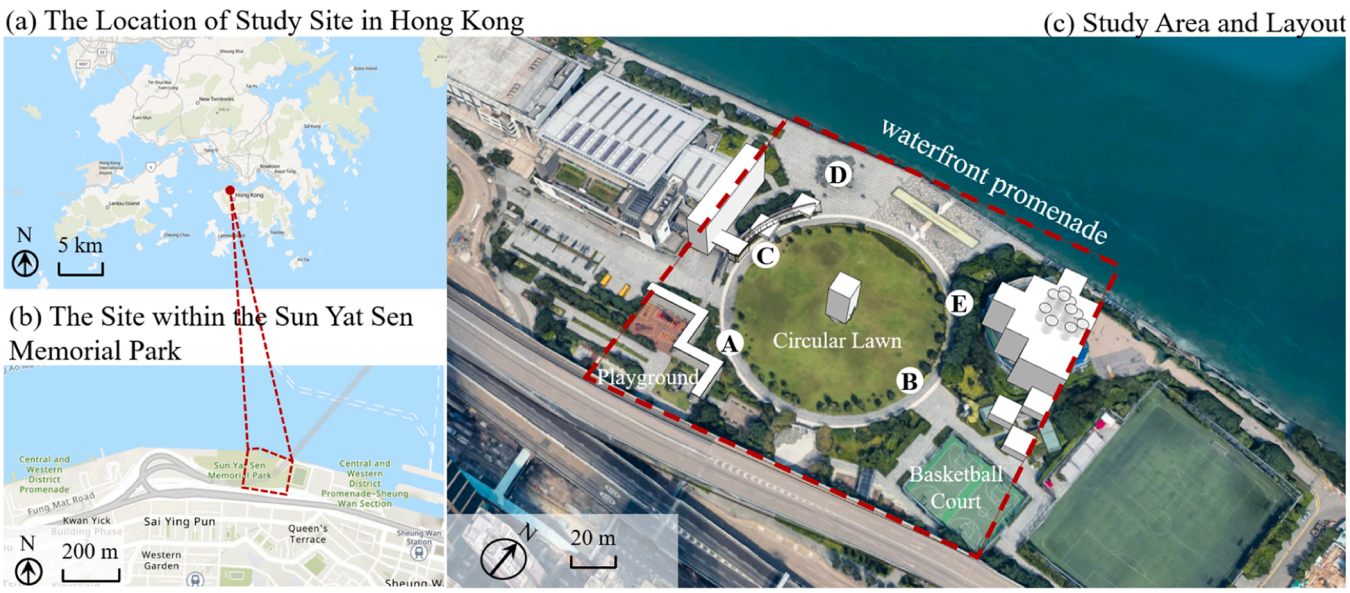

Fig. 3. (a) Location of the study site in Hong Kong; (b) The study site in Sun Yat-Sen Memorial Park; (c) The study area and layout including five measurement locations denoted from A to E.

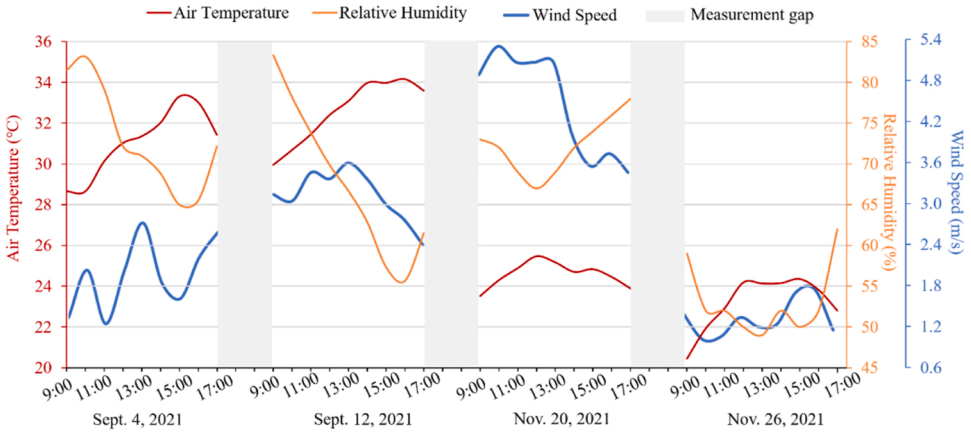

Fig. 4. A summary of ambient air temperature, relative humidity, and wind speed condition at the Meteorological Station from Hong Kong Observatory on four selected days during the field study in 2021.

humidity (RH) and wind speed (V_a) (Eq. (10)). The calculation was implemented using a six-order polynomial approximation algorithm developed by Brode and Wojtach (2010).

$$UTCI = f(T_{mrt}, T_a, V_a, RH) \tag{10}$$

For comparison, an ENVI-met model was built with the same resolution and properties of urban surfaces as the tree simulation model. EVNI-met 5.0 Lite version (ENVI-met, 2023), a free trial license, was used to simulate the cooling effects of trees in terms of air temperature. Due to the limitation of the free version, trees were modeled using simple plants, defined by plant height and ten-layer leaf area density. Details on the model setup and technical parameters of the simulation are provided in the Appendix.

3.2. Tree location optimization

The locations of trees in a park have been coded mathematically in Cartesian Coordinate System; their locations can be denoted and solved as a set of optimization problems.

Consider the following notations:

i = index of potential tree locations.

I = set of all potential tree locations in the study area after removing unsuitable/unavailable areas.

p = number of trees to locate.

$f(\ \ )$ = the microclimate simulation model to calculate the human thermal comfort (UTCI)

$$x_i = \begin{cases} 1 \ if \ \ a \ \ tree \ \ is \ \ located \ \ at \ \ potential \ \ site \ \ i \\ 0 \ otherwise \end{cases}$$

$$Minimize \quad f(x_1, x_2, \ldots\ldots x_i) \tag{11}$$

Subject to:

$$\sum_i x_i = p \tag{12}$$

$$x_i = \{0, 1\} \forall i \in I \tag{13}$$

The objective function is to minimize pedestrian heat stress from planting a p number of trees in the park, as shown in Eq. (11). The design constraints are defined as follows: Eq. (12) defines the number of trees to be planted, where i is the index of potential tree locations; Eq. (13) imposes integer restrictions on the decision variables, where 1(0) means

Table 1
Field experiment schedule at five tree locations and the corresponding zones in the simulation model.

Tree location	Date	Zone ID
A	Sept. 3, 9, and Nov. 19, 2021	132
B	Sept. 4, 12, and Nov. 20, 26, 2021	19
C	Dec. 18, 2021	17
D	Sept. 8, 22, and Dec.9, 11, 2021	11,28,38,50
E	Sept. 15, 18, and Dec. 4, 2021	224

one (no) tree is planted at location *i*.

To obtain the exact solutions for this nonlinear integer programming problem is difficult, due to the computational complexity in both simulation and optimization models. To solve the spatial optimization problem in this study, the genetic algorithm (GA) as a heuristic algorithm was applied. GA, inspired by biological evolution concept, is mimicking species' evolutionary process by selecting highly performing design options, combing cross-over and mutation operation to produce new generations of designs until an optimal option is achieved, as illustrated in the optimal model in Fig. 1. The GA inputs include 1) design variables encoded as integers that correspond to tree locations; 2) design constraints, such as the number of trees, and candidate positions for planting trees within the site excluding the building footprint area; 3) the convergence condition is defined as below: an optimal design solution defined as the reduction of UTCI over baseline (or the status quo) up to 1 °C is obtained, or no improvement observed among individuals after reaching pre-defined maximum generations of a population (20 maximum generations in our analysis); 4) selection rule, survival for fitness, in this case, the tree cooling performance; 5) control parameters of the genetic process, such as population number in each generation, maintain rate that the percentage of individuals can be passed over next process, inbreeding factor determining the similarities degree with parents.

The tree location is mathematically coded by establishing a Cartesian Coordinate System to cover the park site in X, Y, Z dimensions (Fig. 7). Each tree was modeled as a uniform cell with a defined canopy dimension and height, and the candidate position *j* for a tree was specified as a unique set of coordinates $\left(x_j, y_j, z_j\right)$. The design options (individuals) were the possible combinations of tree candidates (genes), referred to as corresponding tree layouts. Fig. 7 shows all candidate positions for trees within the site, excluding the constrained positions such as hardscape paving and buildings.

3.3. Field study & model setup

Field studies have been conducted in a large urban park in Hong Kong to evaluate the Tree Canopy Model. The same park was then used as a case study to test the performance of tree location optimization.

The study site was in the Sun Yat-Sen Memorial Park in Hong Kong (22.29° N, 114.15° E). It is a large urban park bounded by Victoria Harbour to the north, and a major flyover (elevated highway) to the south. The study area measures approximately 30,000 m^2 (Fig. 3) in size and contains 55 mature trees, pavement, and a few buildings.

Table 2
Technical description of the sensors used in field studies.

Parameter (Sensor)	Measurement range	Accuracy	Resolution
Temperature/Relative Humidity Sensor (S-THC-M008)	-40 ~ + 75 ℃	± 0.20 °C, ± 2.5%RH	0.02 °C, 0.01% RH
Solar Radiation Sensor (S-LIB-M003)	0–1280 W/m^2	± 5%	1.25 W/m^2
Wind Speed Sensor (S-WSB-M003)	0 ~76 m/s	± 1.1 m/s	0.5 m/s
Wind Direction Sensor (S-WDA-M003)	0 ~ 355°	± 5°	1.4°

Field measurements were conducted between September and December 2021, covering both hot and cool weather conditions. Measurements were scheduled daily from 9:00–17:00, which is the main period when the park is used the most. Daily weather conditions on four representative days selected as September 4, 12 and November 20, 26 are plotted in Fig. 4. The conditions ranged from being hot and humid in September to cool and drier in November. A considerable variation of wind speed is also observed, ranging from 1 m/s on November 26, up to 5.5 m/s on November 20. A detailed measurement schedule is shown in Table 1.

On-site meteorological data were collected using an Onset HOBO RX3000 weather monitoring station, which was rotated among five locations (A-E) under tree canopies during the study period to capture the variety of thermal conditions influenced by nearby trees (Fig. 5). The weather station included a Temperature/Relative Humidity Sensor (S-THC-M008), a Solar Radiation Sensor (S-LIB-M003), and a set of Wind Speed and Direction Sensors (S-WSB-M003, S-WDA-M003), all mounted to a tripod at 1.5 m above the ground. Sensor recordings were stored in a HOBO data logger at 5 min intervals. Details and the range of accuracy of the sensors are summarized in Table 2.

Concurrent weather data were obtained from the Hong Kong Observatory's ground-based weather station networks, which were used as inputs for the tree simulation model and further evaluated by comparing the predicted results with the measured ones. The solar radiation, wind speed, and wind direction data were obtained from the King's Park Station (22°18′43″N, 114°10′22″E), the closest station with such data available. The air temperature and relative humidity data were obtained from the Hong Kong Observatory station (Fig. 6).

The Tree Canopy Model and Optimization algorithms have been applied to the same study area in search of optimal tree locations in cooling performances. The model configuration, boundary conditions, and optimization objectives are specified below.

The model space has been configured according to the layout of the study site (Fig. 7). The 3D urban geometries, including building, pavement, ground lawn, and trees were acquired from the official

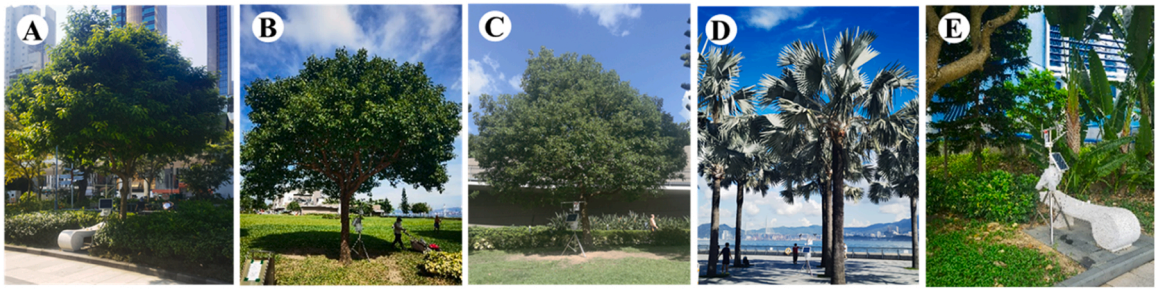

Fig. 5. A view of five measurement locations under tree canopies. A: a sterculia tree; B: a camphor tree; C: a camphor tree; D: an array of nine palm trees, E: a cuban bast tree.

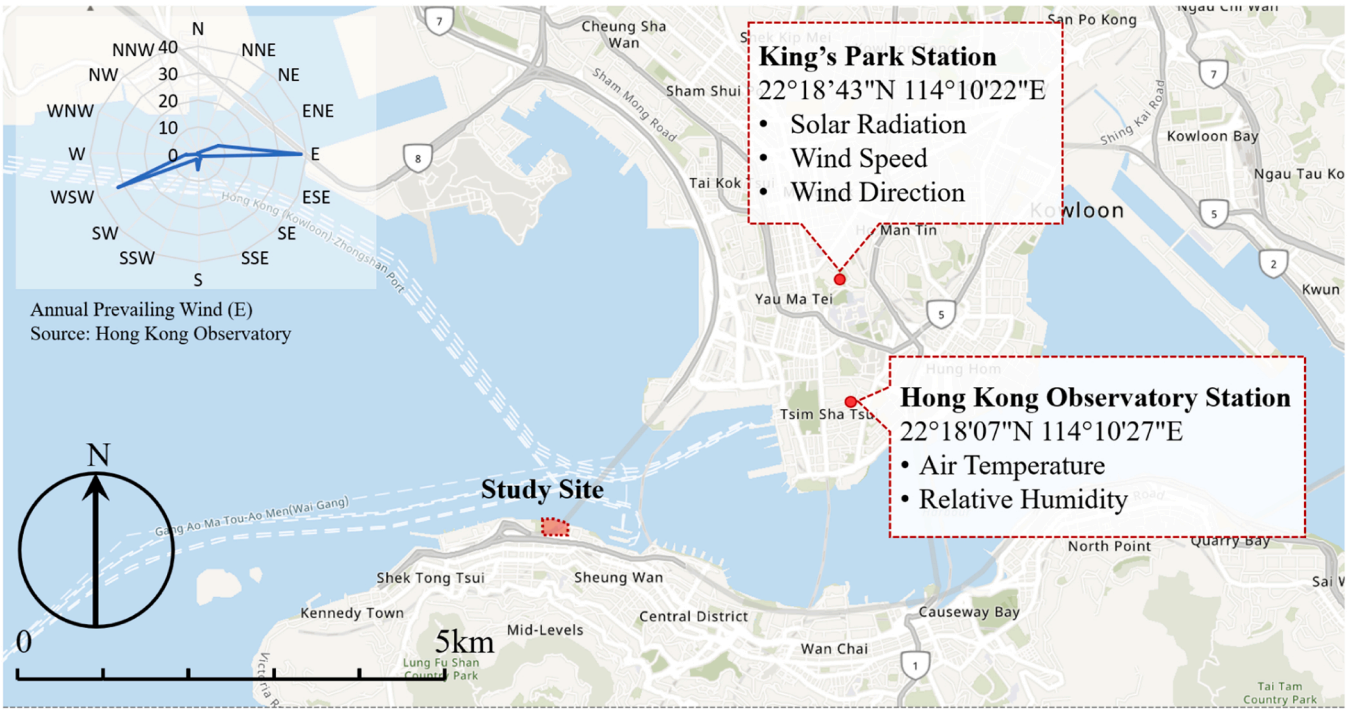

Fig. 6. Location of the study site relative to ground-based weather stations through which ambient meteorological data were obtained (Source: Google Map and Hong Kong Observatory).

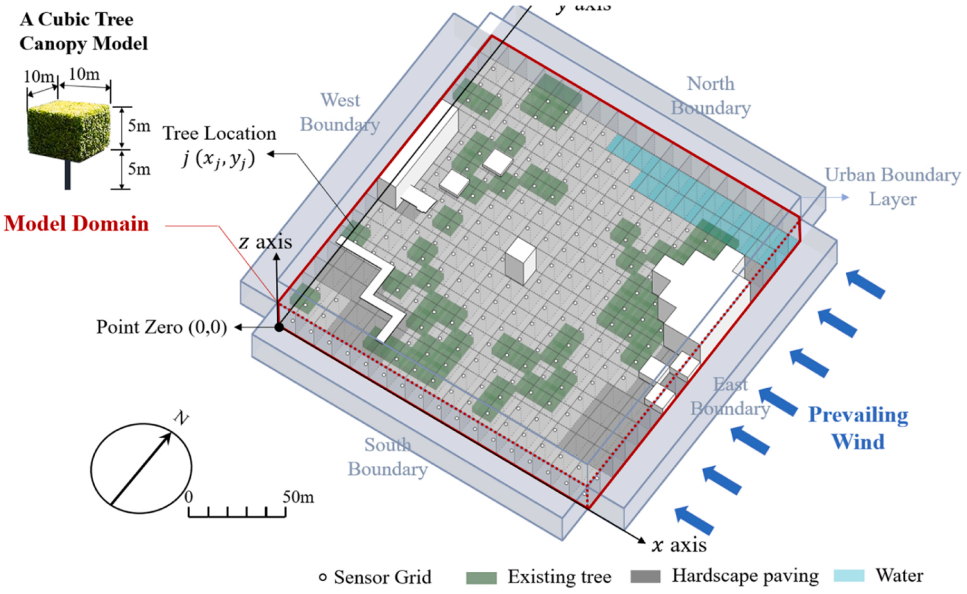

Fig. 7. The model domain, 3D building, zone geometries, and boundary conditions used in this study.

database of the Lands Department of the Hong Kong government (HKLD, 2016). The model domain was divided evenly into 289 identical zones, following a 17 by 17 checkerboard pattern. Each zone measures 10 m (length) × 10 m (width)× 20 m (height). A total of 55 zones were defined as "tree zones" based on the location of the 55 mature trees on-site. They were specified as porous media with restricted connections with the nearby zones. Another 19 zones were specified as "building zones", which overlaps with the existing 3D building massing. A total of five boundary zones were added to the top, east, west, south, and north of the site domain. A sensor point was placed inside each ground-level zone at 1.5 m above the ground, based on which the mean radiant temperature, zonal temperature, wind speed, humidity, and human heat stress were calculated.

The boundary condition consists of pressure, temperature, and humidity. The pressure boundary, including the static and dynamic air pressure conditions, was modeled using a CFD model. The CFD model domain was defined as a volume of (670 m, 670 m, and 300 m in length, width, and height), covering the urban park and its immediate surroundings. The input parameters consist of ambient atmospheric pressure, wind speed, and wind directions derived from the nearby weather station. To simplify, an easterly wind direction and velocity of 3.8 m/s at the height of 10 m were used as inputs, identified based on the annual hourly meteorological record. The vertical wind speed profiles were adjusted using Eq. (13), in which the input wind pressure (P_{v_z})at the

Table 3
Description of Optimization Scenarios with Distinct Number of Trees and Objectives.

Scenario Name	# of Trees	Objective
Coolest Spot (Tree Rearrangement)	55	The coolest possible spot on-site Minimize $UTCI_{min}$
Minimum Average On-Site Heat Stress (Tree Rearrangement)	55	The minimum average on-site UTCI
Most Effective Tree Addition	80	Minimize $UTCI_{mean}$
Maximum Average On-Site Heat Stress (Tree Rearrangement)	55	The maximum average on-site UTCI
Least Effective Tree Addition	80	Maximize $UTCI_{mean}$

boundary surfaces of the model domain was estimated using those measured at the 10 m level ($P_{v_{10}}$)

$$P_{v_{10}} = \xi \frac{{p_{v_{10}}}^2}{2} \tag{14}$$

The CFD model was then executed using FlowDesigner 10.0, a commercial CFD software (AKL, 2020), assuming adiabatic conditions, i.e., no heat transfer between the air and solid surfaces. The outputs are pressure coefficients at the surfaces of the model domain, which are extracted and used as inputs for the Tree Canopy Model. The temperature and humidity boundaries were estimated from those measured from the Hong Kong Observatory weather station (22°18'07"N 114°10'27"E, Fig. 6).

A total of two optimization scenarios were established as design constraints. The first is to rearrange the existing 55 trees on-site to minimize heat stress. Although this is hypothetical in nature, the outcome is useful to inform the magnitude of cooling benefits to be expected if all trees were planted in the "right locations", without additional cost in planting and maintaining new trees. In this case, the number of trees was therefore fixed at 55, yet their locations were

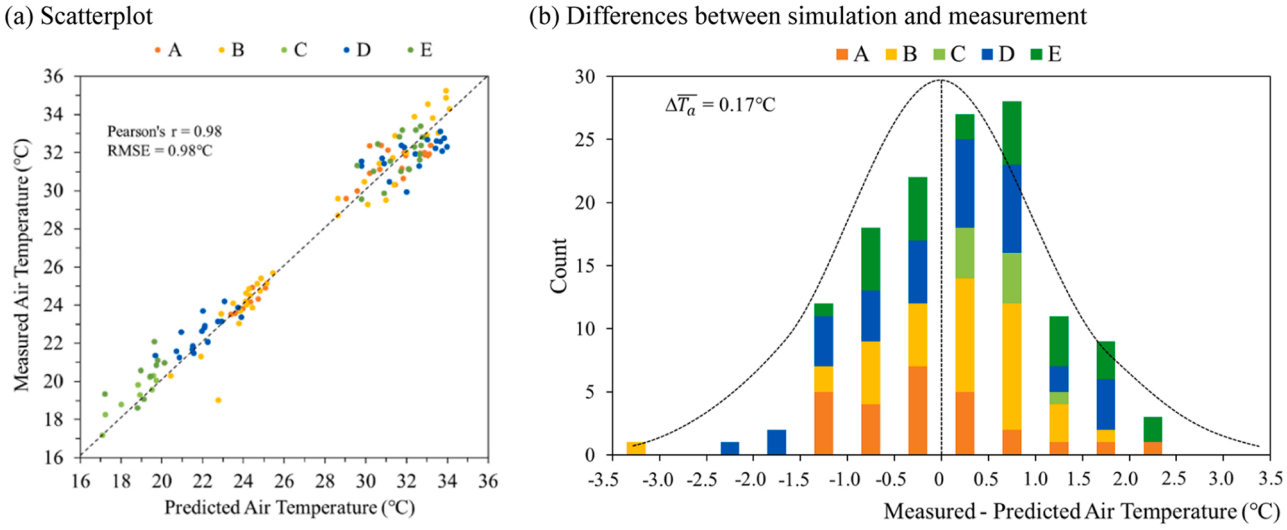

Fig. 8. For the proposed tree simulation model, (a) Scatterplot of measured and predicted air temperature and (b) the differences between simulation and measurement data.

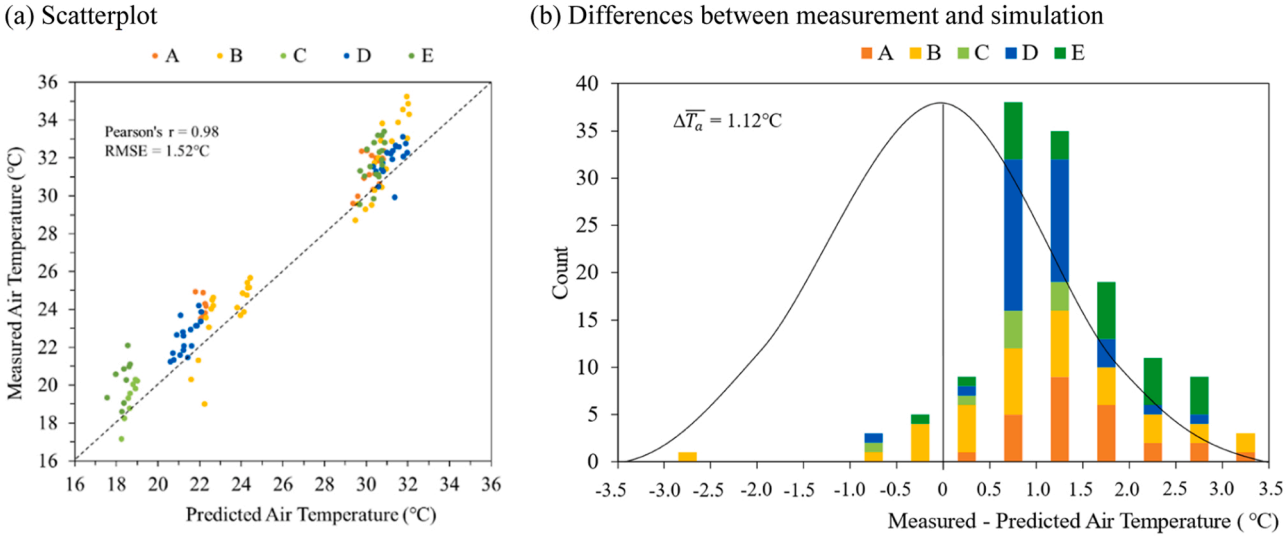

Fig. 9. For ENVI-met, (a) Scatterplot of measured and predicted air temperature and (b) the differences between simulation and measurement data.

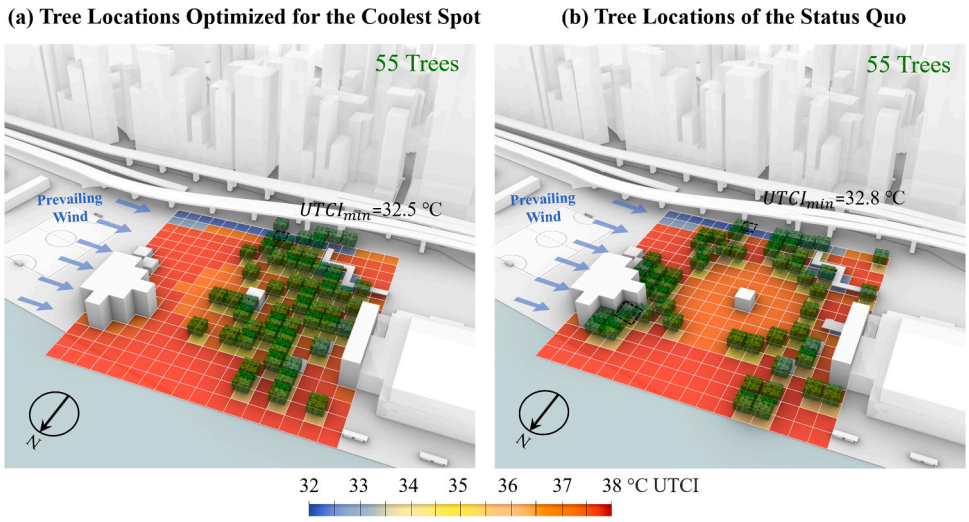

Fig. 10. A comparison of (a) tree locations optimized for the "Coolest Spot", i.e., to minimize $UTCI_{min}$ and (b) tree locations of the status quo.

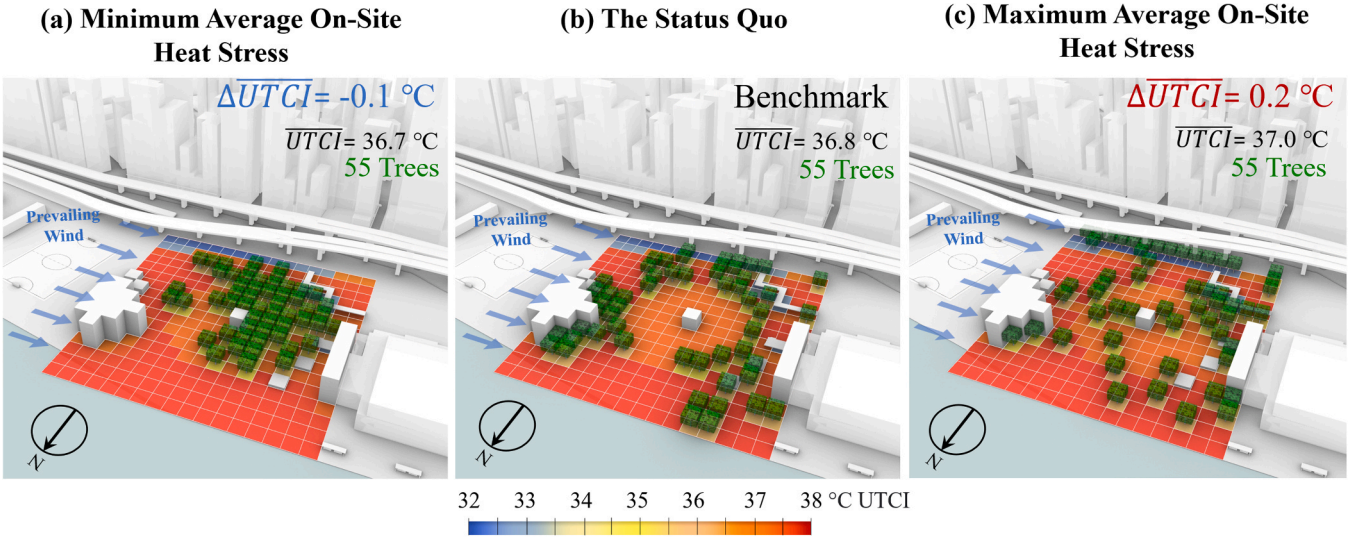

Fig. 11. (a) Tree locations optimized to achieve the minimum on-site heat stress, (b) tree locations of the status quo, and (c) tree locations optimized to achieve the maximum average on-site heat stress.

allowed to vary within the 17 by 17 checkerboard. In a second optimization scenario, 25 new trees are to be added to the site, while the existing 55 trees are expected to stay in the same locations. This scenario is more realistic in guiding the planning of new trees, and it reflects the local policy recommendation of increasing urban tree coverage from 20% to 30%.

Two performance objectives were used to optimize tree locations. The first is to minimize the UTCI equivalent temperature of the coolest spot on-site, and the second is to minimize the average on-site UTCI equivalent temperature (excluding those contained by buildings). To avoid simulating hourly conditions for an extended period, noon on September 12, 2021, was chosen as the time of assessment, representing typical conditions during the summer season. This simplification, although with uncertainties, allows for indicative results on optimal tree layout for cooling benefits. Two additional objectives were also included to identify the 'worst conditions', i.e., the tree locations with the highest level of occupant heat stress. A summary of the total of six optimization scenarios, with their objective functions and the number of allowable trees, is provided in Table 3.

The Genetic Algorithm was configured with the initial design options as 1000, and 100 per new generation of location variations. The maintain rate, that is, the percentage of design options to be maintained into the next generation was set at 15%, and the inbreeding factor, the ratio of difference among design options at 0.75. Model convergence is considered to have been achieved if no simulated reduction in $UTCI_{min}$ or $\overline{UTCI}$ occurs over 20 generations.

4. Results and discussion

The simulated air temperature from the tree model has been compared with measurement data collected during field studies. The near-optimal tree locations under various scenarios, i.e., design constraints and objectives, were obtained and compared with each other. The strength and limitations of the new method are discussed, together with its practical implications.

4.1. Model evaluation

A reasonably good agreement was observed between the measured air temperature on-site and simulated values in the tree model. A Pearson's r of 0.98 and a Root Mean Square Error (RMSE) of 0.98 °C

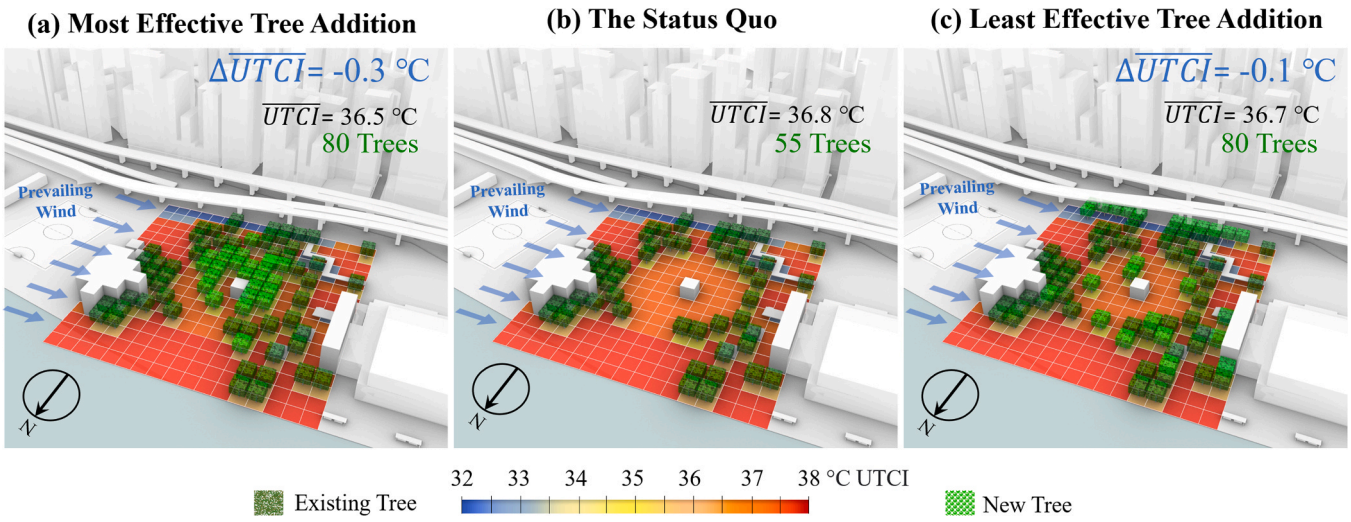

Fig. 12. (a) Locations of 25 new trees optimized to achieve the minimum site average heat stress ($\overline{UTCI}$), (b) locations of the 55 trees in the status quo, and (c) locations of 25 new trees optimized to achieve the maximum site average heat stress ($\overline{UTCI}$).

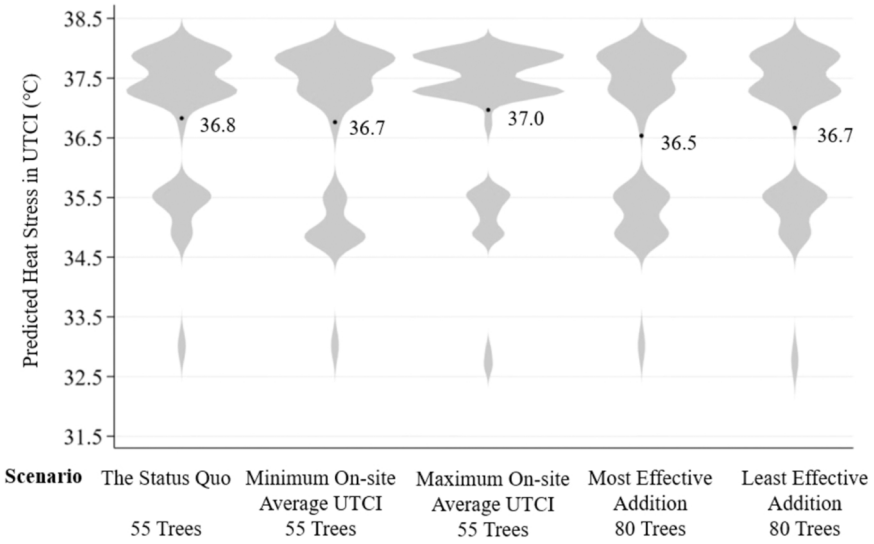

Fig. 13. A violin plot comparing the cooling performances of scenarios in terms of distribution of on-site UTCT under the Lowest Site Average Heat scenario for rearranging existing 55 trees and adding 25 new trees for the study site. In each violin, the black dot indicates the average value.

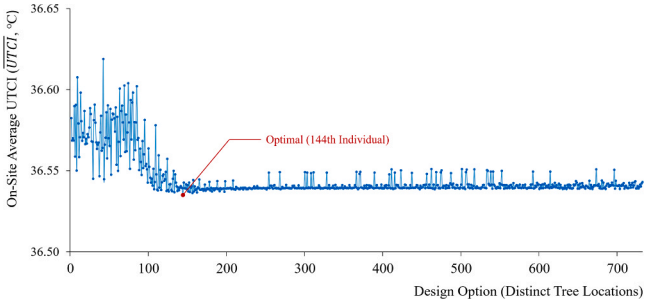

Fig. 14. The optimization process of the Tree Addition Scenario, which aims to minimize the on-site average UTCI ($\overline{UTCI}$) by adding additional 25 trees in the park.

(Fig. 8(a)) are observed between the two, suggesting a close agreement. Notice that the scatterplots appeared on both sides of the 45-degree line for each measurement location (A-E), suggesting that such agreement is consistent across the five locations during this study. The differences between simulated and measured values are plotted in Fig. 8(b), which are normally distributed, with a mean difference $\Delta\overline{T_a}$ of 0.17℃ (Fig. 9 (a)), suggesting that the model neither underestimates nor overestimates air temperature in a systematic manner. Again, such differences are

Table A1
Technical parameters of ENVI-met model.

Item	Input parameter
Size of Simulation Case	21 × 21 × 5
# of grid	2,205
Dynamic time step (s)	1
Boundary Conditions	Simple forcing of 24-cycle of air temperature and humidity, daily average wind speed and localized solar adjustment factor.
Output intervals (s)	600

Table A2
Localized material properties of constructions and tree characteristics.

Construction & Tree	Item	Input Parameter
Building wall	Thickness (m)	0.35
	Albedo of surface (ratio)	0.35
	Surface emissivity (ratio)	0.95
	Heat capacity (J/kg K)	750
	Heat transmission coefficient (W/m^2 K)	0.6
Ground pavement	Albedo of surface (ratio)	0.4
	Surface emissivity (ratio)	0.85
	Heat capacity (J/kg K)	880
	Heat transmission coefficient (W/m^2 K)	0.6
Tree	Canopy height (m)	10
	Canopy width (m)	10
	Leaf area index (m^2/m^2)	2.5
	Albedo (ratio)	0.2
	Leaf emissivity (ratio)	0.92
	Leaf transmittance (ratio)	0.3

consistent across the five measurement locations, suggesting that the simulation model showed no systematic bias for any of the measurement locations and as a whole.

The performance of the ENVI-met, a popular software tool among researchers in this field, is provided for comparison in Fig. 9. It has largely underestimated the air temperature under the study conditions, with a Pearson's r of 0.98 and the RMSE of 1.52 ℃ (Fig. 9(a)). Such underestimation, by about one degree, was consistently found amongst the five measurement locations (Fig. 9(b)). This finding echoes with those from similar studies published recently by Liu et al. (2021) and Ou et al.(2022), which also found the tendency of ENVI-met in underestimating air temperature. One paper suggests the reason being that ENVI-met might have miscalculated the level of solar radiation reaching plant surfaces (Liu et al., 2021). Details on the setup and parameters of ENVI-met simulation are provided in the Appendix.

4.2. Optimization results

The proposed method can suggest possibilities to 'rearrange' the 55 trees on-site to alleviate heat stress under the study conditions. Tree locations, shown in green boxes, are overlaid on top of the simulated UTCI value at each sensor grid, and the zones covered under tree canopies can be some 3 °C cooler than those without in general (Fig. 10). The optimized location under the 'Coolest Spot' scenario is shown in Fig. 10 (a), in comparison with those of the status quo (Fig. 10 (b)). Concentrating trees on the leeward side of the site tends to cool down the park more than the sparsely distributed trees of the status quo. The 'coolest spot' of the former measures at $UTCI_{min}$ = 32.5 ℃, compared with those of the latter at 32.8 ℃, a 0.3 ℃ reduction. The coolest spots in both scenarios were found at the southern edge of the park, under the shadows of the highway, known locally as the flyover. This single cooling spot has behavioral significance, as one can argue that its presence allows occupants to move around and settle in cooler locations in a park during heat waves, referred to as heat-coping in behavioral literature (Wilhelmi et al., 2010). Results suggest that more cooling can be expected if a similar park was to be built anew, although such rearrangement is usually impractical for mature trees in an existing park.

Trees can also be relocated to minimize the average on-site heat stress level. Their locations optimized with respect to the objective of minimizing the $\overline{UTCI}$ are illustrated in Fig. 11 (a), in comparison with UTCI of the status quo in Fig. 11 (b). The difference in on-site average UTCI can be 0.1 ℃ between the two. Further, the tree locations have been optimized to achieve the 'worst outcomes', i.e., the highest level of heat stress. The results are shown in Fig. 11 (c), in which the UTCI is 0.2 ℃ higher than those of the status quo. The differences between the best and the worst outcomes, i.e., the $\overline{UTCI}$ between Fig. 11 (a) and (c), are statistically significant, with a one-on-one t-test score of − 1.61 (p = 0.05), rejecting the null hypothesis that the group means are identical. The 'worst outcome' with 'wrong' tree locations can exacerbate heat stress, although this may be useful for parks in cold climates, in which warmer outdoor spaces are desirable. The results suggest that better cooling can be achieved by concentrating trees at the center toward the leeward side of the site, whereas spreading trees sparsely tends to yield higher levels of heat stress on average.

The method can also support decisions to plant new trees. The results are shown in Fig. 10, with 25 new trees added to the site in response to the local policy of increasing urban green coverage from 20% to 30%. The most effective locations to plant new trees, optimized to minimize the $\overline{UTCI}$, are shown in (Fig. 12 (a)); The benchmark is again the status quo (Fig. 12 (b)). The cooling benefit associated with these new trees, measured by the difference of $\overline{UTCI}$ between the two can be 0.3 ℃, with a t-test score of 2.3 (p = 0.01) rejecting the null hypothesis that the two values are equal.

Further, the locations for new trees can also be optimized for the 'least effective' outcomes. The results are shown in Fig. 12 (c), with the predicted $\overline{UTCI}$ at 36.7 ℃, a mere 0.1 ℃ reduction of 0.1 ℃ from the status quo, or a third of the cooling benefits expected from Fig. 12 (a) with the same number of trees. Interestingly, the cooling benefit of 80 trees in their 'least effective' locations is on par with the optimal rearrangement for the 55 trees in Fig. 11 (a). In other words, fewer trees in 'optimal' locations can do the same job as what is expected from more. Findings from this study are consistent with others that the cooling benefits of trees can be enhanced by rearranging them, as much as from adding new trees (Milošević et al., 2017; Morakinyo and Lam, 2016). In the 'most effective' case, the newly added trees tend to concentrate at the center of the site, which was previously unshaded, whereas in the least effective case, the new trees seem to be spreading sparsely across the site. This is yet another support for the earlier findings that trees are to be concentrated in their locations to enhance their cooling benefits under the study condition.

A comparison of cooling performance of various design scenarios is plotted in Fig. 13. A violin plot is used, which shows the peak, the mean, the median, the interquartile range, and the overall distribution of simulated UTCI at each grid. For each scenario, the data distribution follows an undulate shape and the wave crests reflect different design features, i.e., shading and paving types. From top to bottom, the first and second wave crest indicate the unshaded hard paving and central lawn areas, the third indicates the tree-shaded hard paving, the fourth indicates tree-shaded lawn area; while the fifth peak shows the coolest locations, which are shaded by both trees and flyover, with additional breeze induced by nearby buildings. An optimized tree layout for cooling purposes, as it is shown for both scenarios (rearranging 55 trees or adding 25 new trees), can increase the proportions of the third and the fourth crests, while reducing the proportions of the first two.

Computation-wise, the proposed method has performed satisfactorily in reaching the cooling performance convergence, that is, the ability to identify optimal tree locations within a reasonable period. An example is shown in Fig. 12, which shows the optimization process under the Tree Addition scenario. The simulated on-site heat stress measured by average UTCI ($\overline{UTCI}$) has been plotted against design options (tree locations). The objective function appears to have been steadily descending toward a lower value, and the optimal design occurred at the 144th option, when the simulated $\overline{UTCI}$ reached 36.5 ℃. The genetic algorithm has kept running till the 732th option, and the model has been regarded as having reached the performance convergence, i.e., the lack of further progress over an extended period.Fig. 14.

4.3. Discussion

This study has contributed to the tree modeling and optimization literature. A novel method, empowered by simulation models and genetic algorithms, can systematically identify tree layouts to further reduce human heat stress in outdoor spaces. The approach outlined in

this paper can drive the design process toward the optimum, and converge with improved cooling performances, thus integrating the performance evaluation into the scenario-based decision-making process and saving precious time in professional landscape design practice.

The strength of the proposed method is its reliability and computational efficiency. The proposed tree simulation model considers the full sets of components of tree cooling mechanisms, from shading and evapotranspiration to modification of wind. Simulated results yielded satisfactory agreements with measurement data, with no systematic biases observed under the study conditions. Its performance was better in comparison with that of the ENVI-met, a popular software tool amongst researchers in this field. Our results showed that ENVI-met tends to underestimate the on-site air temperature, which echoes findings from other studies using similar approaches (Liu et al., 2021; Ouyang et al., 2022) The proposed method also runs reasonably fast, which takes three mins to predict an hourly condition for the park site used in this study. For an optimization run, it took seven hours on an ordinary desktop computer (Intel Processor i9–10900 CPU @ 2.80 GHz, 64 GB RAM, Nvidia GeForce RTX 3070, 8 GB), including identifying the optimal tree layout from 700 + alternatives before reaching a convergence (Fig. 12). This computational efficiency is an added advantage in policy and professional design practices, where decisions are usually made under demanding deadlines.

The practical implications of this study lie at both the policy and landscape design levels. At the policy level, guidelines on tree locations may be as important as mandating their numbers. Simulated evidence has suggested that trees planted at optimized locations can deliver a similar amount of cooling as more trees (see Figs. 9 & 10). Specifying a lump-sum green coverage ratio, as has been practiced in many urban forestry policies to guide greenery provision at the city level, may not be sufficient for the placement of individual trees. Results from this study also suggest that, at the landscape design level, concentrating tree canopies on the leeward side toward the prevailing wind can further enhance their cooling performances under the study conditions. With greenery in its 'right place', the park can be cooler with the same number of trees. The difference between the 'best' and the 'worst' tree locations can be up to 0.3 °C in UTCI equivalent temperature. It is a small difference, but it is above the Just Noticeable Difference (JND) threshold in human thermal sensation of 0.09 °C, which has been established by Lee et al. (1998) based on indoor experiment data. Although such JND threshold is absent in terms of UTCI equivalent temperature in an outdoor space, we consider the indoor JND as indicative to the outdoors, if not directly comparable, since human body respond to changes in the thermal environment following the same neurophysiological pathway, i.e., skin thermoreceptors detect the temperature and its changes, and the synthesis of such signals in the brain. Thus, the reduction of some 0.3 °C in park UTCI equivalent temperature, on average, should be regarded as meaningful, and the findings can reinforce our message that trees should be planted in the 'right places' in order to maximize their cooling potentials, and such right places depend on climate, user preferences, and tree locations should be customized for each site given the constraints and context.

The study is limited in several aspects. First, the case application in an urban park relies on considerable simplifications, such as the uniform zone division and the assumed discrete tree locations, not to mention that all tree canopies were treated as cubic geometries of identical size, transmissivity, and porosity. Second, findings from this study should not be automatically extended to another climate or location; further tests are needed to determine the extent of applicability of the study findings. Third, the tree simulation model needs further evaluation in terms of humidity, wind speed, thermal comfort, etc. The impacts of the water body on cooling benefits also need to be taken into consideration. Lastly, the use of a genetic algorithm may only identify the local optimal, rather than a global optimal. In other words, we cannot prove mathematically that the 'true' optimal tree locations have been obtained in the current approach.

The next step is to analyze the impacts of tree species with varying leaf area density, canopy size, and trunk height on cooling performances and their optimal locations. The geometrical setting of the tree model can be refined to accommodate more details, such as the minimum setback distance between buildings and trees, as well as between trees themselves. The tree simulation model can be further evaluated using measured wind speed, moisture, and radiative datasets obtained under tree canopies. The tree simulation model and the optimization algorithms are programmed using Python script on top of the Rhinoceros and Grasshopper platform, and they have the potentials to be further developed into a software tool in support of policy and landscape design practices.

5. Conclusion

In this paper, a novel method has been developed to search for the optimal tree locations regarding their cooling performances in outdoor spaces. It is based on a physics-based simulation model, which has been partially evaluated using field measurement data collected from a large urban park during cool, temperate, and hot seasons, with satisfactory agreements between predicted and measured air temperature. It can automatically identify tree locations to maximize their cooling benefits while accounting for design constraints, such as avoidance of existing buildings and utilities. It has been tested in the same urban park with promising results. It can identify the optimal layout to rearrange the existing 55 trees, hypothetically, which is expected to yield a site-average cool benefit of up to 0.3 ℃ in UTCI equivalent temperature, compared with the 'worst layout'. Trees can provide the most cooling if they are concentrated on the leeward side of the park relative to the prevailing wind, rather than spread evenly. Findings suggest that having greenery in its 'right place' may be just as important as having enough trees, and this has important implications for urban forestry policy. The proposed method can inform research and landscape design practices concerning park cooling as a goal.

CRediT authorship contribution statement

Tongping Hao: writing of the first draft, field experiment, data curation, data analysis, figures and data visualization. **Qunshan Zhao:** concept, research design, methods - optimization, manuscript editing and revision, **Jianxiang Huang:** concept, research design, methods - simulation, manuscript editing and revision, resource, supervision.

Declaration of Competing Interest

The authors declare that they have no known competing financial interests or personal relationships that could have appeared to influence the work reported in this paper.

Acknowledgment

The research is supported by two grants from the National Natural Science Foundation of China (#51978594 & #51708473). The study is also funded in part by the Hong Kong Research Grants Council Theme-Based Research Scheme under Grant T22–504/21-R and by the ESRC's ongoing support for the *Urban Big Data Centre* (UBDC) [ES/L011921/1 and ES/S007105/1]. The authors want to thank the anonymous reviewers for their insightful comments and suggestions on an earlier version of this manuscript.

Appendix

The ENVI-met simulation model was built with the same spatial resolution and properties of urban surfaces as the proposed tree simulation model. EVNI-met 5.0 Lite version (ENVI-met, 2023), a free trial license, was used to simulate the cooling effects of trees in terms of air

temperature. The technical parameters of the ENVI-met model are provided in Table A1. The detailed localized values of constructions and trees were listed in Table A2.

References

AKL, 2020. FlowDesigner: Software Development for Air Flow / Thermal Environment Analysis.

Allen, R.G., Pereira, L.S., Raes, D., Smith, M., 1998. Guidelines for Computing Crop Water Requirements, FAO Irrigation and Drainage Paper. Food and Agriculture Organization of the United Nations (FAO), Rome.

Ansys Fluent, 2022. Ansys Fluent [WWW Document]. URL https://www.ansys.com/products/fluids/ansys-fluent (accessed Jul.11.2022).

Bajsanski, I., Stojakovic, V., Jovanovic, M., 2016. Effect of tree location on mitigating parking lot insolation. Comput. Environ. Urban Syst. 56, 59–67. https://doi.org/10.1016/J.COMPENVURBSYS.2015.11.006.

Bean, A., Alperi, R.W., Federer, C.A., 1975. A method for categorizing shelterbelt porosity. Agric. Meteorol. 14, 417–429. https://doi.org/10.1016/0002-1571(74)90035-1.

Brode, P., Wojtach, B., 2010. UTCI Calculator [WWW Document]. URL http://www.utci.org/utcineu/utcineu.php (accessed Apr.20.2022).

Bruse, M., Fleer, H., 1998. Simulating surface-plant-air interactions inside urban environments with a three dimensional numerical model. Environ. Model. Softw 13, 373–384.

Buccolieri, R., Santiago, J.L., Rivas, E., Sanchez, B., 2018. Review on urban tree modeling in CFD simulations: aerodynamic, deposition and thermal effects. Urban For. Urban. Green 31, 212–220. https://doi.org/10.1016/J.UFUG.2018.03.003.

Chen, H., Ooka, R., Kato, S., 2008. Study on optimum design method for pleasant outdoor thermal environment using genetic algorithms (GA) and coupled simulation of convection, radiation and conduction. Build. Environ. 43, 18–30. https://doi.org/10.1016/j.buildenv.2006.11.039.

Cheung, P.K., Fung, C.K.W., Jim, C.Y., 2020. Seasonal and meteorological effects on the cooling magnitude of trees in subtropical climate. Build. Environ. 177. https://doi.org/10.1016/j.buildenv.2020.106911.

City of Barcelona, 2017. Trees for Life: Master Plan for Barcelona's Trees (2017 - 2037). Àrea d'Ecologia Urbana. Ajuntament de Barcelona., Barcelona.

City of Melbourne, 2012. Urban Forest Strategy: Making a great city greener 2012–2032, City of Melbourne. Melbourne.

City of Phoenix, 2010. Tree and Shade Master Plan. Phoenix.

Duursma, R.A., Medlyn, B.E., 2012. MAESPA: A model to study interactions between water limitation, environmental drivers and vegetation function at tree and stand levels, with an example application to [CO_2] × drought interactions. Geosci. Model Dev. 5, 919–940. https://doi.org/10.5194/gmd-5-919-2012.

ENVI-met, 2023. ENVI-met 5.0 LITE [WWW Document]. URL https://www.envi-met.com/buy/#license-models-5.

Fan, C., Wang, Z., 2020. Spatiotemporal characterization of land cover impacts on urban warming: A spatial autocorrelation approach. Remote Sens. https://doi.org/10.3390/rs12101631.

Hao, T., Huang, J., He, X., Li, L., Jones, P., 2022. A machine learning-enhanced design optimizer for urban cooling. Indoor Built Environ. 32 https://doi.org/10.1177/1420326×221112857.

HKG, 2022. Greening Hong Kong [WWW Document]. URL https://www.gov.hk/en/residents/environment/sustainable/greening/greening.htm (accessed Jul.29.2022).

HKLD, 2016. Digital Maps [WWW Document]. Hong Kong Lands Dep. URL https://www.landsd.gov.hk/en/survey-mapping/mapping/multi-scale-topographic-mapping/digital-map.html (accessed Apr.1.2022).

Huang, J., Cedeño-Laurent, J.G., Spengler, J.D., 2014. CityComfort+: a simulation-based method for predicting mean radiant temperature in dense urban areas. Build. Environ. 80, 84–95. https://doi.org/10.1016/j.buildenv.2014.05.019.

Huang, J., Hao, T., Wang, Y., Jones, P., 2022. A street-scale simulation model for the cooling performance of urban greenery: evidence from a high-density city. Sustain. Cities Soc. 82, 103908 https://doi.org/10.1016/j.scs.2022.103908.

Jendritzky, G., de Dear, R., Havenith, G., 2012. UTCI-Why another thermal index. Int. J. Biometeorol. 56, 421–428. https://doi.org/10.1007/s00484-011-0513-7.

Krayenhoff, E.S., Christen, A., Martilli, A., Oke, T.R., 2014. A multi-layer radiation model for urban neighbourhoods with trees. Bound. -Layer. Meteor. 151, 139–178. https://doi.org/10.1007/s10546-013-9883-1.

Krayenhoff, E.S., Santiago, J.L., Martilli, A., Christen, A., Oke, T.R., 2015. Parametrization of drag and turbulence for urban neighbourhoods with trees. Bound. -Layer. Meteor. 156, 157–189. https://doi.org/10.1007/s10546-015-0028-6.

Krayenhoff, E.S., Jiang, T., Christen, A., Martilli, A., Oke, T.R., Bailey, B.N., Nazarian, N., Voogt, J.A., Giometto, M.G., Stastny, A., Crawford, B.R., 2020. A multi-layer urban canopy meteorological model with trees (BEP-Tree): street tree impacts on pedestrian-level climate. Urban Clim. 32, 100590 https://doi.org/10.1016/j.uclim.2020.100590.

Kuala Lumpur City Hall, 2021. Kuala Lumpur Climate Action Plan 2050. Kuala Lumpur.

Lachapelle, J.A., Krayenhoff, E.S., Middel, A., Meltzer, S., Broadbent, A.M., Georgescu, M., 2021. A microscale three-dimensional model of urban outdoor thermal exposure (TUF-Pedestrian). Int. J. Biometeorol. https://doi.org/10.1007/s00484-022-02241-1.

Lee, H.M., Cho, C.K., Yun, M.H., Lee, M.W., 1998. Development of a temperature control procedure for a room air- conditioner using the concept of just noticeable difference (JND) in thermal sensation. Int. J. Ind. Ergon. 22, 207–216. https://doi.org/10.1016/S0169-8141(97)00009-7.

Li, Y., Song, Y., 2019. Optimization of vegetation arrangement to improve microclimate and thermal comfort in an urban park. Int. Rev. Spat. Plan. Sustain. Dev. 7, 18–30. https://doi.org/10.14246/irspsd.7.1_18.

Li, Y., Fan, S., Li, K., Zhang, Y., Dong, L., 2021. Microclimate in an urban park and its influencing factors: a case study of Tiantan Park in Beijing, China. Urban Ecosyst. 24, 767–778. https://doi.org/10.1007/s11252-020-01073-4.

Lindberg, F., Grimmond, C.S.B., 2011. The influence of vegetation and building morphology on shadow patterns and mean radiant temperatures in urban areas: model development and evaluation. Theor. Appl. Climatol. 105, 311–323. https://doi.org/10.1007/s00704-010-0382-8.

Liu, Z., Cheng, W., Jim, C.Y., Morakinyo, T.E., Shi, Y., Ng, E., 2021. Heat mitigation benefits of urban green and blue infrastructures: a systematic review of modeling techniques, validation and scenario simulation in ENVI-met V4. Build. Environ. 200, 107939 https://doi.org/10.1016/j.buildenv.2021.107939.

Mak, M.Y., Ng, S.T., 2005. The art and science of Feng Shui - a study on architects' perception. Build. Environ. 40, 427–434. https://doi.org/10.1016/j.buildenv.2004.07.016.

Meili, N., Acero, J.A., Peleg, N., Manoli, G., Burlando, P., Fatichi, S., 2021. Vegetation cover and plant-trait effects on outdoor thermal comfort in a tropical city. Build. Environ. 195 https://doi.org/10.1016/j.buildenv.2021.107733.

Milošević, D.D., Bajšanski, I.V., Savić, S.M., 2017. Influence of changing trees locations on thermal comfort on street parking lot and footways. Urban . Urban Green. 23, 113–124. https://doi.org/10.1016/j.ufug.2017.03.011.

Morakinyo, T.E., Lam, Y.F., 2016. Simulation study on the impact of tree-configuration, planting pattern and wind condition on street-canyon's micro-climate and thermal comfort. Build. Environ. 103, 262–275. https://doi.org/10.1016/j.buildenv.2016.04.025.

Morakinyo, T.E., Ouyang, W., Lau, K.K.L., Ren, C., Ng, E., 2020. Right tree, right place (urban canyon): tree species selection approach for optimum urban heat mitigation - development and evaluation. Sci. Total Environ. 719, 137461 https://doi.org/10.1016/j.scitotenv.2020.137461.

Ng, E., Ren, C., 2018. China's adaptation to climate & urban climatic changes: a critical review. Urban Clim. 23, 352–372. https://doi.org/10.1016/j.uclim.2017.07.006.

Ng, E., Chen, L., Wang, Y., Yuan, C., 2012. A study on the cooling effects of greening in a high-density city: an experience from Hong Kong. Build. Environ. 47, 256–271. https://doi.org/10.1016/j.buildenv.2011.07.014.

Nice, K.A., Coutts, A.M., Tapper, N.J., 2018. Development of the VTUF-3D v1.0 urban micro-climate model to support assessment of urban vegetation influences on human thermal comfort. Urban Clim. 24, 1052–1076. https://doi.org/10.1016/j.uclim.2017.12.008.

Oke, T.R., 1989. The micrometeorology of the urban forest. Philos. Trans. - R. Soc. Lond., B 324, 335–349. https://doi.org/10.1098/rstb.1989.0051.

OpenFOAM, 2022. OpenFOAM [WWW Document]. URL https://www.openfoam.com/ (accessed Jul.11.2022).

Ouyang, W., Sinsel, T., Simon, H., Morakinyo, T.E., Liu, H., Ng, E., 2022. Evaluating the thermal-radiative performance of ENVI-met model for green infrastructure typologies: experience from a subtropical climate. Build. Environ. 207, 108427 https://doi.org/10.1016/J.BUILDENV.2021.108427.

Park, C.Y., Lee, D.K., Krayenhoff, E.S., Heo, H.K., Ahn, S., Asawa, T., Murakami, A., Kim, H.G., 2018. A multilayer mean radiant temperature model for pedestrians in a street canyon with trees. Build. Environ. 141, 298–309. https://doi.org/10.1016/j.buildenv.2018.05.058.

Park, C.Y., Yoon, E.J., Lee, D.K., Thorne, J.H., 2020. Integrating four radiant heat load mitigation strategies is an efficient intervention to improve human health in urban environments. Sci. Total Environ. 698, 134259 https://doi.org/10.1016/j.scitotenv.2019.134259.

Patra, R., 2009. Vaastu shastra: towards sustainable development. Sustain. Dev. 17, 244–256. https://doi.org/10.1002/sd.388.

PHOENICS, 2022. PHOENICS [WWW Document]. URL https://www.cham.co.uk/phoenics.php (accessed Jul.11.2022).

Redon, E., Lemonsu, A., Masson, V., 2019. An urban trees parameterization for modeling microclimatic variables and thermal comfort conditions at street level with the Town Energy Balance model (TEB-SURFEX v8.0). Geosci. Model Dev. 13, 385–399. https://doi.org/10.5194/gmd-13-385-2020.

SG, 2021. Singapore Green Plan 2030 [WWW Document]. Singapore Gov. URL https://www.greenplan.gov.sg/ (accessed Apr.20.2022).

Stojakovic, V., Bajsanski, I., Savic, S., Milosevic, D., Tepavcevic, B., 2020. The influence of changing location of trees in urban green spaces on insolation mitigation. Urban . Urban Green. 53 https://doi.org/10.1016/j.ufug.2020.126721.

Toparlar, Y., Blocken, B., Maiheu, B., van Heijst, G.J.F., 2017. A review on the CFD analysis of urban microclimate. Renew. Sustain. Energy Rev. 80, 1613–1640. https://doi.org/10.1016/j.rser.2017.05.248.

Wallenberg, N., Lindberg, F., Rayner, D., 2022. Locating trees to mitigate outdoor radiant load of humans in urban areas using a metaheuristic hill-climbing algorithm - introducing TreePlanter v1.0. Geosci. Model Dev. 15, 1107–1128. https://doi.org/10.5194/gmd-15-1107-2022.

Wong, N.H., Tan, C.L., Kolokotsa, D.D., Takebayashi, H., 2021. Greenery as a mitigation and adaptation strategy to urban heat. Nat. Rev. Earth Environ. 2, 166–181. https://doi.org/10.1038/s43017-020-00129-5.

Yang, A.S., Juan, Y.H., Wen, C.Y., Chang, C.J., 2017. Numerical simulation of cooling effect of vegetation enhancement in a subtropical urban park. Appl. Energy 192, 178–200. https://doi.org/10.1016/j.apenergy.2017.01.079.

Yang, Y., Gatto, E., Gao, Z., Buccolieri, R., Morakinyo, T.E., Lan, H., 2019. The "plant evaluation model" for the assessment of the impact of vegetation on outdoor microclimate in the urban environment. Build. Environ. 159, 106151 https://doi.org/10.1016/j.buildenv.2019.05.029.

Yuan, C., Norford, L., Ng, E., 2017. A semi-empirical model for the effect of trees on the urban wind environment. Landsc. Urban Plan. 168, 84–93. https://doi.org/10.1016/j.landurbplan.2017.09.029.

Zhang, J., Gou, Z., 2021. Tree crowns and their associated summertime microclimatic adjustment and thermal comfort improvement in urban parks in a subtropical city of China. Urban . Urban Green. 59 https://doi.org/10.1016/j.ufug.2020.126912.

Zhang, L., Zhan, Q., Lan, Y., 2018. Effects of the tree distribution and species on outdoor environment conditions in a hot summer and cold winter zone: a case study in Wuhan residential quarters. Build. Environ. 130, 27–39. https://doi.org/10.1016/j.buildenv.2017.12.014.

Zhao, Q., Myint, S.W., Wentz, E.A., Fan, C., 2015. Rooftop surface temperature analysis in an urban residential environment. Remote Sens. https://doi.org/10.3390/rs70912135.

Zhao, Q., Wentz, E.A., Murray, A.T., 2017. Tree shade coverage optimization in an urban residential environment. Build. Environ. 115, 269–280. https://doi.org/10.1016/j.buildenv.2017.01.036.

Zhao, Q., Sailor, D.J., Wentz, E.A., 2018. Impact of tree locations and arrangements on outdoor microclimates and human thermal comfort in an urban residential environment. Urban . Urban Green. 32, 81–91. https://doi.org/10.1016/j.ufug.2018.03.022.